Matching of experimental and statistical-model thermonuclear reaction rates at high temperatures

J. R. Newton, R. Longland, and C. Iliadis
Department of Physics and Astronomy, University of North Carolina, Chapel Hill, North Carolina, 27599-3255, USA and Triangle Universities Nuclear Laboratory, Durham, North Carolina 27708-0308, USA
(Received 11 April 2008; published 19 August 2008)

We address the problem of extrapolating experimental thermonuclear reaction rates toward high stellar temperatures ($T > 1$ GK) by using statistical model (Hauser-Feshbach) results. Reliable reaction rates at such temperatures are required for studies of advanced stellar burning stages, supernovae, and x-ray bursts. Generally accepted methods are based on the concept of a Gamow peak. We follow recent ideas that emphasized the fundamental shortcomings of the Gamow peak concept for narrow resonances at high stellar temperatures. Our new method defines the *effective thermonuclear energy range* (ETER) by using the 8th, 50th, and 92nd percentiles of the cumulative distribution of fractional resonant reaction rate contributions. This definition is unambiguous and has a straightforward probability interpretation. The ETER is used to define a temperature at which Hauser-Feshbach rates can be matched to experimental rates. This matching temperature is usually much higher compared to previous estimates that employed the Gamow peak concept. We suggest that an increased matching temperature provides more reliable extrapolated reaction rates since Hauser-Feshbach results are more trustworthy the higher the temperature. Our ideas are applied to 21 (p,γ), (p,α), and (α,γ) reactions on $A = 20$–40 target nuclei. For many of the cases studied here, our extrapolated reaction rates at high temperatures differ significantly from those obtained using the Gamow peak concept.

DOI: 10.1103/PhysRevC.78.025805 PACS number(s): 26.20.−f, 24.60.−k, 26.50.+x, 97.10.Cv

I. INTRODUCTION

Thermonuclear reaction rates at high temperatures ($T >$ 1 GK) are required for the modeling of advanced stellar burning stages, supernovae, and x-ray bursts. It is straightforward to estimate such rates if the necessary ingredients—nonresonant and broad-resonance cross sections, resonance energies and strengths—are known experimentally [1]. However, for a number of reasons, any experiment has an associated cutoff at some maximum bombarding energy, $E_{\rm max}^{\rm exp}$. For example, the value of $E_{\rm max}^{\rm exp}$ may be dictated by the highest energy attainable with the particle accelerator; or the measurement is simply terminated at a bombarding energy where the data analysis becomes untractable, perhaps because resonances start to overlap strongly so that a resonance structure is not discernible anymore. At lower stellar temperatures, where the *effective thermonuclear energy range* (ETER) is entirely covered by experiment, the value of $E_{\rm max}^{\rm exp}$ is inconsequential. However, with increasing temperature a point is eventually reached where the reaction rates cannot be calculated anymore using the available experimental information alone since part of the ETER has shifted beyond $E_{\rm max}^{\rm exp}$.

In such situations, the established procedure is as follows. The ETER is identified with the Gamow peak, whose location and (Gaussian approximation) $1/e$ width are given by [1]

$$E_0 = 0.1220\left(Z_0^2 Z_1^2 \frac{M_0 M_1}{M_0 + M_1} T_9^2\right)^{1/3} \text{(MeV)}, \quad (1)$$

$$\Delta E_0 = 0.2368\left(Z_0^2 Z_1^2 \frac{M_0 M_1}{M_0 + M_1} T_9^5\right)^{1/6} \text{(MeV)}, \quad (2)$$

where M_i and Z_i are the masses (in u) and charges of projectile and target and T_9 is the plasma temperature in GK. Note that 84% of the area under a Gaussian is enclosed between the $1/e$ points. It is apparent from these expressions that for increasing temperature the Gamow peak shifts toward higher energy and becomes broader. Based on this concept, a "matching" temperature can be determined according to

$$E_0\left(T_{\rm match}^{\rm GP}\right) + n\Delta E_0\left(T_{\rm match}^{\rm GP}\right) = E_{\rm max}^{\rm exp}, \quad (3)$$

with n denoting an empirical parameter ($n = 1$ is used most frequently). For temperatures $T < T_{\rm match}^{\rm GP}$ the reaction rates are assumed to be based on experimental input alone, because the predominant fraction of the Gamow peak is located in the experimentally investigated energy region. At $T > T_{\rm match}^{\rm GP}$ a substantial fraction of the Gamow peak is located beyond $E_{\rm max}^{\rm exp}$ and insufficient experimental information is available for calculating the total rates. For the latter case, statistical model (Hauser-Feshbach) reaction rates are renormalized to match the experimental rates at a temperature of $T_{\rm match}^{\rm GP}$. The renormalized Hauser-Feshbach reaction rates then provide the recommended reaction rates in the temperature region $T > T_{\rm match}^{\rm GP}$. This strategy has not only been adopted in the most recent evaluations of charged-particle thermonuclear reaction rates [2,3] but represents, in lack of an alternative so far, the established procedure in the field of nuclear astrophysics.

It must be remembered that the concept of a Gamow peak is based on the assumption of a nonresonant reaction cross section [1]. However, at higher temperatures the total reaction rates for nuclei in the $A = 12$–40 range are almost always dominated by contributions from narrow resonances. It turns out that, under certain conditions, the Gamow peak concept is also useful for narrow resonances, as has been pointed out by Fowler and Hoyle [4]: resonances located in the region of the Gamow peak are thought to provide a much larger contribution to the total rate compared to other resonances. In fact, the Gamow peak concept is widely used in nuclear

astrophysics because it represents a simple and straightforward method for identifying the most important resonances in a given thermonuclear reaction.

Recently it has been demonstrated by Newton *et al.* [5] that the Gamow peak concept for narrow resonances breaks down under conditions that are especially favorable to higher temperatures. We will not repeat the discussion of Ref. [5] here but instead will focus in the following on specific examples to make the main ideas transparent. The reaction rate contribution of narrow resonances (in units of $\mathrm{cm}^3\ \mathrm{mol}^{-1}\ \mathrm{s}^{-1}$) is given by [1]

$$N_A\langle\sigma v\rangle = \frac{1.5399\cdot 10^{11}}{\left(\frac{M_0 M_1}{M_0+M_1}\,T_9\right)^{3/2}}\sum_i (\omega\gamma)_i e^{-11.605\,E_i/T_9}, \qquad (4)$$

where i labels different resonances, E_i and $(\omega\gamma)_i$ are the resonance energy and strength in units of MeV, and M_i are the relative atomic masses of projectile and target in u. At higher bombarding energies of interest here, the quantities E_i and $(\omega\gamma)_i$ can be directly obtained in the laboratory, for example, from measured thick-target yields [1]. From Eq. (4) one may naively expect that those resonances with the largest value of $(\omega\gamma)_i$ and, at the same time, the smallest value of E_i may dominate the total reaction rate. However, this simplistic consideration does not take into account that $(\omega\gamma)_i$ is itself energy dependent. The strength of a resonance is defined in terms of partial widths as

$$\omega\gamma = \frac{2J+1}{(2j_0+1)(2j_1+1)}\frac{\Gamma_a\Gamma_b}{\Gamma}, \qquad (5)$$

with J, j_0, j_1 the spins of resonance, projectile and target, respectively, and Γ_a, Γ_b, Γ the partial widths of the entrance channel, exit channel, and the total width, respectively. Consider as a simple case a reaction with only two energetically allowed channels, a particle channel and the γ-ray channel. The partial widths associated with these channels have vastly different energy dependences. The partial width for a charged particle a (usually either a proton or α particle) is strongly energy dependent because the projectile must penetrate the Coulomb and centripetal barriers. The energy dependence is given by $\Gamma_a \sim P_\ell(E)$, where $P_\ell(E)$ is the penetration factor for an orbital angular momentum of ℓ. The penetration factor determines the energy-dependence of charged-particle partial widths: they vary by many orders of magnitude, from vanishingly small values at very low bombarding energies to values in excess of many keV at higher energies. However, γ-ray partial widths depend only weakly on the interaction energy via $\Gamma_\gamma \sim E_\gamma^{2L+1}$, where E_γ and L are the energy and multipolarity, respectively, of the γ-ray transition under consideration. The total γ-ray partial width is then given by the sum over all contributing transitions. Typical values of the total γ-ray partial width amount to ≈meV–eV.

As an example, we will now present numerical results that are obtained under certain simplifying assumptions: (i) we consider proton capture ($M_0 = 1.0078$ and $Z_0 = 1$) on a target with a mass and charge of $M_1 = 25$ and $Z_1 = 12$, respectively; (ii) only s-wave ($\ell = 0$) resonances that decay via dipole radiation ($L = 1$) are considered; (iii) we chose the same spectroscopic factor, $C^2S = 0.01$, for all resonances considered;[1] (iv) the Q value for this hypothetical reaction is assumed to be in excess of several MeV so that the energy dependence of the γ-ray partial width can be disregarded (because $E_\gamma = Q + E_i$ for the primary ground-state transition); a constant value of $\Gamma_\gamma = 1$ eV is chosen for the total γ-ray partial width; (v) all spins are set equal to unity for simplicity. For these assumptions, the energies and strengths of nine resonances in the range of $E_i = 20-180$ keV are shown in Fig. 1(a) as red bars. The solid black line represents the Gamow peak at a temperature of $T = 0.06$ GK. The resonance strengths obviously become larger for increasing energies because the transmission through the Coulomb barrier

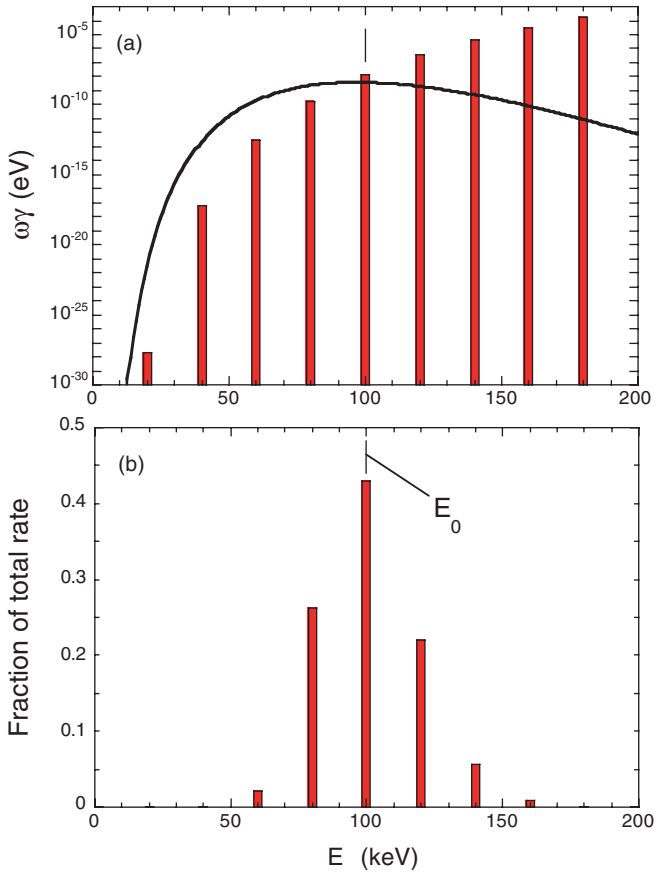

FIG. 1. (Color online) Narrow resonance reaction rate contributions at a temperature of $T = 0.06$ GK for proton capture on a hypothetical target. See text for details. (a) Resonance strengths (red bars) and Gamow peak (black solid line); (b) fractional contribution of each resonance to the total reaction rate; E_0 labels the location of the Gamow peak maximum.

[1]The proton partial width is given by $\Gamma_p(E) = 2[\hbar^2/(\mu R^2)]P_\ell(E)\theta_{\mathrm{sp}}^2 C^2 S$, with μ, R, and θ_{sp}^2 the reduced mass, interaction radius, and dimensionless reduced single-particle width, respectively [1]. We do not wish to imply that the spectroscopic factors are (nearly) equal for all resonances in an actual reaction, which is obviously not the case. The point of our simplifying assumptions is to focus attention on the energy-dependent quantities that enter into the expressions for reaction rates.

increases. For all of the resonances displayed in Fig. 1(a) the condition $\Gamma_a \ll \Gamma_\gamma$ holds so that, according to Eq. (5), the proton partial width determines entirely the resonance strength, i.e., $\omega\gamma \approx \omega\Gamma_a$. Because Γ_a contains the information on the transmission through the Coulomb barrier, the Gamow peak concept applies in this case: resonances located in the Gamow peak, $E_0 \pm \Delta E_0/2 = 100 \pm 25$ keV, will be most important for the total reaction rate, whereas those located outside this energy range are unimportant. These qualitative arguments are supported quantitatively by Fig. 1(b), showing the actual fractional contribution of each resonance to the total reaction rate. Clearly, the distribution peaks at the center of the Gamow peak, E_0.

It is interesting to consider now a much higher temperature. For exactly the same assumptions that are discussed above, the energies and strengths of 19 resonances in the range of $E_i = 200$–2000 keV are shown in Fig. 2(a) as red bars. The solid black line represents again the Gamow peak, this time at a temperature of $T = 2$ GK. Only for the lowest two resonances, $E_i = 200$ and 300 keV, is the condition $\Gamma_a \ll \Gamma_\gamma$ fulfilled. For the resonances at higher energies the increased transmission

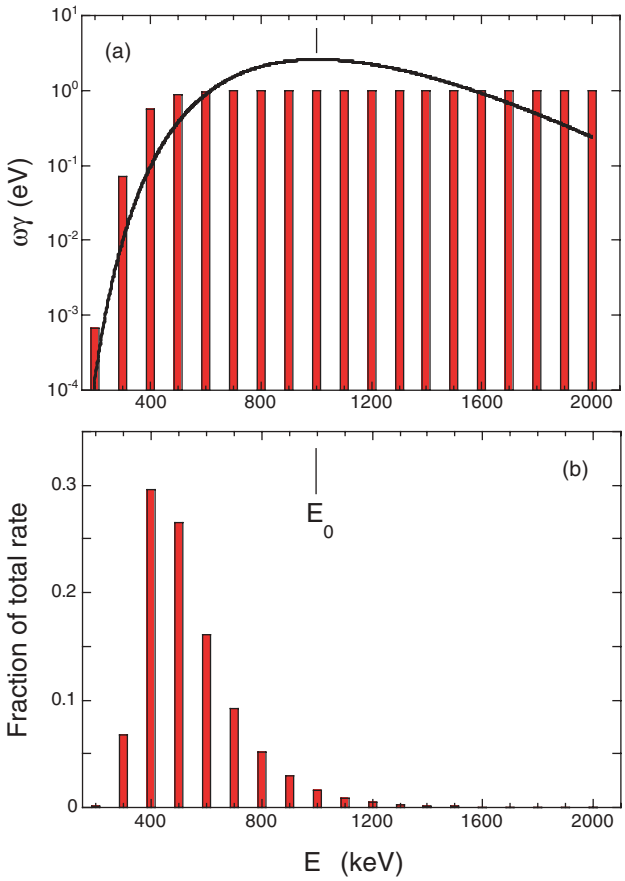

FIG. 2. (Color online) Narrow resonance reaction rate contributions at a temperature of $T = 2$ GK for proton capture on a hypothetical target. See text for details. (a) Resonance strengths (red bars) and Gamow peak (black solid line); (b) fractional contribution of each resonance to the total reaction rate; E_0 labels the location of the Gamow peak maximum.

through the Coulomb barrier gives rise to relatively large values of Γ_a, so that we obtain either $\Gamma_a \approx \Gamma_\gamma$ (for $E_i = 400$ keV) or $\Gamma_a \gg \Gamma_\gamma$ (for $E_i > 400$ keV). In the latter case, the total γ-ray partial width determines entirely the resonance strength, $\omega\gamma \approx \omega\Gamma_\gamma$, and $\omega\gamma$ assumes a constant value for our assumptions. Because the penetration through the Coulomb barrier is inconsequential for the resonance strength, a Gamow peak does not exist. These qualitative arguments are supported quantitatively by Fig. 2(b), showing again the actual fractional contribution of each resonance to the total reaction rate. This time the largest contributions arise form the resonances at $E_i = 400$, 500, and 600 keV (i.e., the lowest-lying resonances that do not fulfill the condition $\Gamma_a \ll \Gamma_\gamma$). Note that the Gamow peak is located at $E_0 \pm \Delta E_0/2 = 1000 \pm 500$ keV, significantly higher in energy than the distribution of the actual fractional reaction rate contributions.

The issue raised above is important in the context of the present work since the Gamow peak concept should not be applied at higher temperatures ($T > 1$ GK) where experimental reaction rates must be extrapolated using Hauser-Feshbach rates. More precisely, the established procedure for determining the matching temperature, Eqs. (1)–(3), is incorrect. In Sec. II we present a new and more reliable method for defining the ETER. Significant differences in energy location and width between the ETER and the Gamow peak will become apparent in Sec. III where we present some of our results. A summary is given in Sec. IV. We emphasize again that the ideas presented here are most important if the total reaction rate at high temperatures is dominated by narrow resonances,[2] which is the case for the majority of thermonuclear reactions in the $A = 12$–40 region. Our methods may not apply to exceptional cases where the total rate at high temperatures is dominated by broad resonances or nonresonant processes. Throughout this work, energies are presented in the center of mass system, unless mentioned otherwise.

II. METHOD

We will discuss first the temperature dependence of the fractional reaction rate contribution for an ensemble of narrow resonances. The results shown in Fig. 3 are obtained for the same assumptions as stated above. Figures 3(a) and 3(b) display the fractional reaction rate distributions at a temperature of $T = 2$ GK and $T = 5$ GK, respectively. The Gamow peak locations for the two temperatures, $E_0 \pm \Delta E_0/2 = 1000 \pm 500$ keV and $E_0 \pm \Delta E_0/2 = 1850 \pm 1000$, respectively, are indicated by the upper horizontal bars. A number of interesting observations can be pointed out. First, the actual distribution (shown as red vertical bars) does not coincide with the Gamow peak location, as already mentioned in Sec. I. Second, the actual distribution of fractional reaction rate contributions shifts slightly toward higher energy with increasing temperature, but the relative shift is much smaller than for the Gamow peak. The weak

[2]A resonance may be called "narrow" if its total width is smaller compared to the width of the ETER.

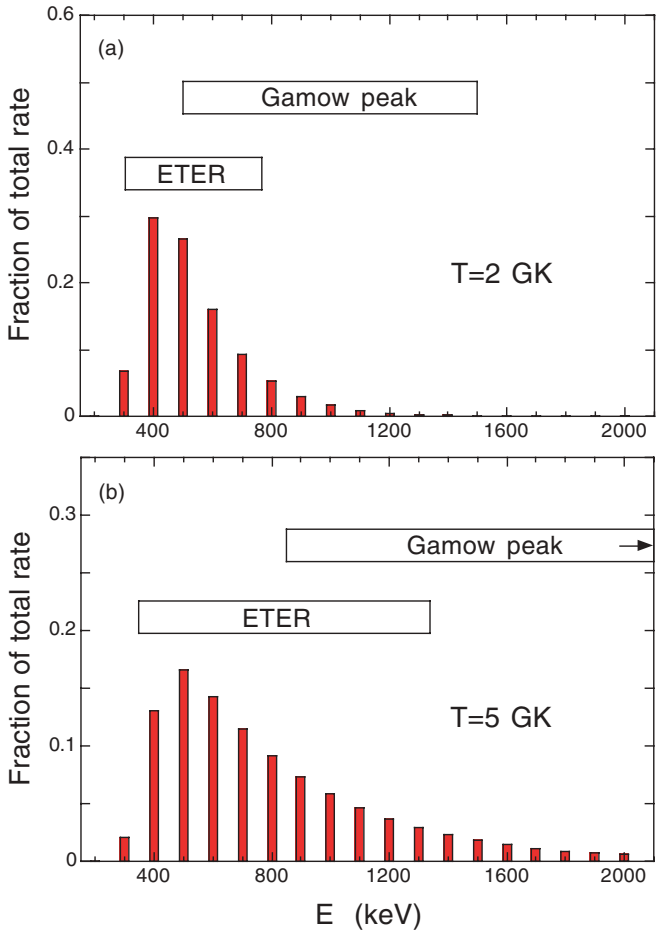

FIG. 3. (Color online) Fractional contributions of narrow resonances to the total reaction rate for proton capture on a hypothetical target. See text. (a) $T = 2$ GK [the distribution is the same as the one shown in Fig. 2(b)]; (b) $T = 5$ GK. The upper horizontal bars indicate the location of the Gamow peak, $E_0 \pm \Delta E_0/2$ [the upper boundary in part (b) is off scale], whereas the lower horizontal bars display the actual effective thermonuclear energy range (ETER).

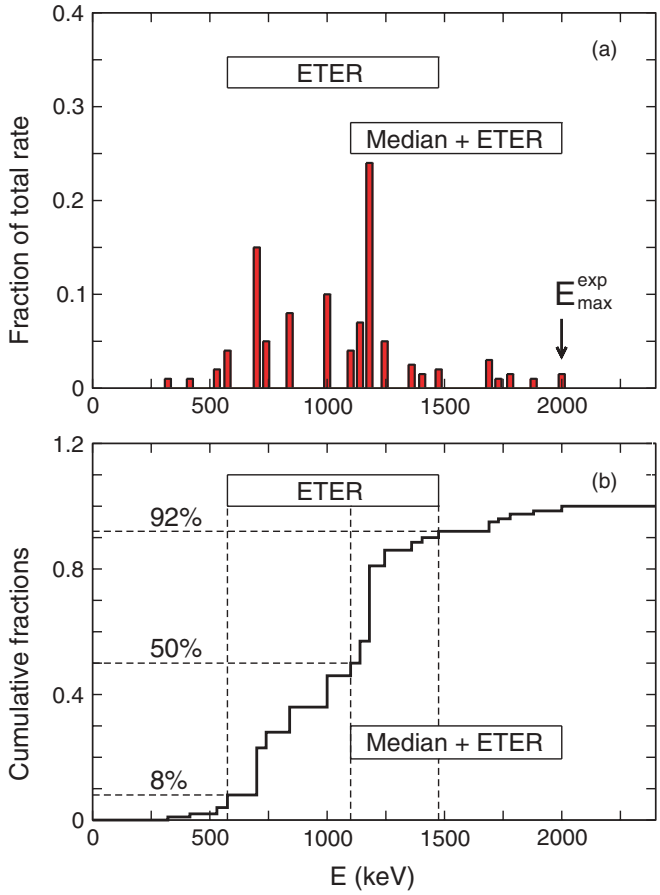

FIG. 4. (Color online) (a) Fractional contributions of narrow resonances to the total reaction rate at a given temperature, T. The highest-lying resonance corresponds to the experimental cutoff energy, $E_{\rm max}^{\rm exp}$; (b) Cumulative distribution of fractional resonant rates; the 8th, 50th, and 92nd percentiles define the ETER (see text). For this particular temperature, Eq. (6) is fulfilled (see lower horizontal bar in panels), i.e., $T = T_{\rm match}^{\rm ETER}$.

energy shift of the actual distribution is explained by the temperature dependence of the reaction rate: according to Eq. (4), the reaction rate maximum for a single resonance of energy E_i is located at $T_9^{\rm max} = 7.737 E_i$, where the resonance energy is in units of MeV. Because the temperature location of the maximum reaction rate is directly proportional to the resonance energy, the relative rate contribution of higher-lying resonances increases (moderately) with rising temperature.

For the reasons given above it is obvious that at elevated temperatures the Gamow peak for narrow resonances must be replaced by a more reliable concept. Clearly, under such conditions the effective thermonuclear energy range (ETER) is defined by the actual distribution of fractional resonant rate contributions, as is apparent from Figs. 1(b), 2(b), and 3. We obtain a quantitative estimate of the ETER in the following manner: (i) the cumulative distribution function of the fractional resonant rates is computed (which resembles a step function); (ii) the 50th percentile of the cumulative distribution, which is equal to the median of the fractional resonant rates, is identified with the energy location of the ETER; (iii) the 8th and 92nd percentiles of the cumulative distribution define an energy range that we identify with the width of the ETER; this range covers an integrated rate fraction of 84%, i.e., the same value as the area enclosed between the $1/e$ points of the (Gaussian approximation of the) Gamow peak. Note that this procedure, which is schematically shown in Fig. 4, is different from the preliminary strategy applied in Newton *et al.* [5]. Our new method requires additional computational efforts but has the advantage of an unambiguous definition and a straightforward probability interpretation. The resulting ETERs for the previously discussed examples are shown in Fig. 3 as the lower horizontal bars in each panel. It is apparent that at both temperatures the ETER has a significantly different energy location and width compared to the conventional region of the Gamow peak.

We are now in a position to address the problem of how to match experimental and Hauser-Feshbach reaction rates. Recall from Sec. I that the matching temperature is generally influenced by the experimental cutoff energy, $E_{\rm max}^{\rm exp}$. Based on the above discussion, we replace the conventional definition

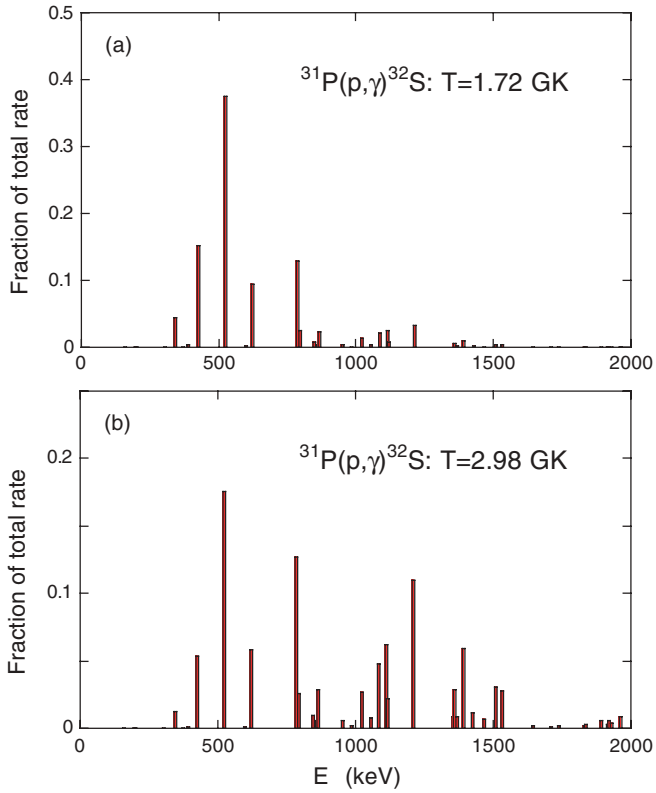

FIG. 5. (Color online) Fractional contributions of narrow resonances to the total rate of the $^{31}\mathrm{P}(p,\gamma)^{32}\mathrm{S}$ reaction. The resonance energies and strengths are from Ref. [6]. (a) $T = 1.72$ GK; (b) $T = 2.98$ GK. These two temperatures correspond to $T^{\mathrm{GP}}_{\mathrm{match}}$ and $T^{\mathrm{ETER}}_{\mathrm{match}}$, respectively, with $E^{\mathrm{exp}}_{\mathrm{max}} \approx 2.0$ MeV for this reaction (Table I).

of a matching temperature, Eq. (3), by

$$E'\left(T^{\mathrm{ETER}}_{\mathrm{match}}\right) + n\Delta E'\left(T^{\mathrm{ETER}}_{\mathrm{match}}\right) = E^{\mathrm{exp}}_{\mathrm{max}}. \tag{6}$$

The quantity $T^{\mathrm{ETER}}_{\mathrm{match}}$ is the matching temperature based on the ETER; E' denotes the location of the ETER, which is determined by the 50th percentile of the cumulative distribution of fractional resonant rate contributions; $\Delta E'$ is the width of the ETER, defined by the 8th and 92nd percentiles such that this region contributes 84% of the total reaction rate. Test calculations show (see below) that a choice of $n = 1$ for the empirical parameter provides sufficiently accurate results. Because at a given value of T the ETER is expected to be located at much *lower* energies compared to the Gamow peak (see Sec. I), the value of our matching temperature, $T^{\mathrm{ETER}}_{\mathrm{match}}$, is significantly *higher* compared to $T^{\mathrm{GP}}_{\mathrm{match}}$.

The situation is schematically displayed in Fig. 4: at a given temperature, T, the ETER (upper horizontal bars) is located well within the experimentally investigated energy region and Eq. (6) is precisely fulfilled (i.e., $E' + \Delta E'$ is equal to the experimental cutoff energy, implying $T = T^{\mathrm{ETER}}_{\mathrm{match}}$; see lower horizontal bars). For smaller temperatures, the ETER shifts to the left and the total reaction rate can be based on experimental information alone. At higher temperatures, the ETER shifts to the right such that resonances located beyond the experimentally investigated energy region may contribute to the total rate. In the latter case, the rate beyond the matching temperature, $T^{\mathrm{ETER}}_{\mathrm{match}}$, must be extrapolated using Hauser-Feshbach results. In the next section, we apply our ideas to a number of realistic cases.

III. RESULTS

Consider as an example the $^{31}\mathrm{P}(p,\gamma)^{32}\mathrm{S}$ reaction for which 42 narrow resonances have been measured up to an energy of $E_r = 1963$ keV [6]. Application of the Gamow peak concept, Eq. (3), results in a matching temperature of $T^{\mathrm{GP}}_{\mathrm{match}} = 1.72$ GK. A significantly higher matching temperature, $T^{\mathrm{ETER}}_{\mathrm{match}} = 2.98$ GK, is deduced from our adopted method, which is based on Eq. (6). The actual distributions of fractional resonant rate contributions at these two temperatures are shown in Fig. 5. At $T = 1.72$ GK (top panel) almost 80% of the total rate is contributed by only four resonances, whereas at $T = 2.98$ GK many more resonances contribute significantly to the total reaction rate. It is obvious that the matching of experimental and Hauser-Feshbach rates is more reliable at the higher temperature where the contribution from many resonances is a prerequisite for the applicability of the statistical theory of nuclear reactions. In fact, the application of the Hauser-Feshbach theory is questionable at the lower temperature of $T = 1.72$ GK.

We have performed similar calculations for a number of reactions, including interactions of the type (p,γ), (p,α), and (α,γ). The results are listed in Table I. Columns 2 and 3 provide information on the number of measured resonances that are taken into account and the measured energy of the highest-lying resonance, respectively. The resonance energies and strengths are adopted from Refs. [6,7], including a number of updates. Our recommended matching temperature $T^{\mathrm{ETER}}_{\mathrm{match}}$, calculated from Eq. (6), is given in column 4. Column 5 lists the commonly used matching temperature $T^{\mathrm{GP}}_{\mathrm{match}}$, which is computed from Eq. (3). It is apparent that $T^{\mathrm{ETER}}_{\mathrm{match}}$ significantly exceeds $T^{\mathrm{GP}}_{\mathrm{match}}$ for most reactions investigated. In a number of cases we find values of $T^{\mathrm{ETER}}_{\mathrm{match}}$ in excess of 10 GK, which usually represents the maximum temperature that is of interest in nuclear astrophysics. Consequently, for these reactions there is no longer a need for matching experimental and theoretical results: their rates up to $T = 10$ GK can be based on experiment alone, in contrast to previous predictions.

It is interesting to explore why $^{31}\mathrm{P}(p,\alpha)^{28}\mathrm{Si}$ and $^{35}\mathrm{Cl}(p,\alpha)^{32}\mathrm{S}$ are the only reactions for which $T^{\mathrm{ETER}}_{\mathrm{match}}$ does not exceed $T^{\mathrm{GP}}_{\mathrm{match}}$. Consider a (p,α) reaction on the same hypothetical target as assumed in Sec. I. If we assume again only s-wave resonances in the proton and α-particle channel, and the same value of $C^2S = 0.01$ for the proton and α-particle spectroscopic factors, then the α-particle partial width, Γ_α, becomes smaller than the proton partial width, Γ_p, for a proton bombarding energy in excess of $E \approx 1.2$ MeV.[3] Beyond this energy, we find $\omega\gamma_{p\alpha} \approx \omega\Gamma_\alpha$ and the proton partial width

[3]The result is based on the ratio of s-wave penetration factors for protons and α particles at the appropriate bombarding energies.

TABLE I. Comparison of matching temperatures based on the ETER and the Gamow peak.

Reaction	n_r [a]	$E_{\max}^{\exp}$ [b] (keV)	$T_{\text{match}}^{\text{ETER}}$ [c] (GK)	$T_{\text{match}}^{\text{GP}}$ [d] (GK)	Rate ratio [e] NON-SMOKER	Rate ratio [f] MOST
^{20}Ne$(\alpha,\gamma)^{24}$Mg	44	5011	10.00	3.22	1.04	0.30
^{21}Ne$(p,\gamma)^{22}$Na	46	1937	8.96	2.23	1.02	0.41
^{22}Ne$(p,\gamma)^{23}$Na	55	1823	4.05	2.05	1.13	0.75
^{23}Na$(p,\gamma)^{24}$Mg	50	2256	10.00	2.56	0.91	0.31
^{23}Na$(p,\alpha)^{20}$Ne	48	2328	3.53	2.67	0.77	0.76
^{24}Mg$(p,\gamma)^{25}$Al	9	2311	9.56	2.49	0.35	0.19
^{24}Mg$(\alpha,\gamma)^{28}$Si	47	5240	10.00	2.97	0.80	0.20
^{25}Mg$(p,\gamma)^{26}$Al	80	1762	3.25	1.73	1.18	0.64
^{26}Mg$(p,\gamma)^{27}$Al	133	2867	4.31	3.32	0.97	0.83
^{27}Al$(p,\gamma)^{28}$Si	105	3819	10.00	4.60	0.91	0.49
^{27}Al$(p,\alpha)^{24}$Mg	90	2967	3.62	3.29	0.96	0.93
^{28}Si$(p,\gamma)^{29}$P	9	2991	10.00	3.16	2.08	1.08
^{29}Si$(p,\gamma)^{30}$P	76	3075	5.05	3.28	0.96	0.66
^{30}Si$(p,\gamma)^{31}$P	93	2929	5.18	3.07	0.70	0.52
^{31}P$(p,\gamma)^{32}$S	42	1963	2.98	1.72	0.92	0.53
^{31}P$(p,\alpha)^{28}$Si	25	1963	1.57	1.72	0.91	0.91
^{32}S$(p,\gamma)^{33}$Cl	14	2470	8.56	2.23	0.13	0.07
^{35}Cl$(p,\gamma)^{36}$Ar	91	2828	5.08	2.57	1.02	0.59
^{35}Cl$(p,\alpha)^{32}$S	94	2838	2.25	2.58	1.09	1.19
^{36}Ar$(p,\gamma)^{37}$K	10	2575	7.39	2.17	0.25	0.15
^{40}Ca$(p,\gamma)^{41}$Sc	8	1887	1.96	1.32	0.40	0.34

[a]Number of narrow resonances taken into account; resonance energies and strengths are from Refs. [6,7], including some updates.

[b]Experimental cutoff energy, i.e., energy of highest measured resonance.

[c]Present temperature for matching experimental and Hauser-Feshbach rates, calculated from Eq. (6); values listed as "10.00 GK" correspond actually to matching temperatures in excess of 10 GK.

[d]Commonly used temperature for matching experimental and Hauser-Feshbach rates, calculated from Eq. (3), which is based on the Gamow peak concept. See text.

[e]Ratio of extrapolated reaction rates using $T_{\text{match}}^{\text{ETER}}$ and $T_{\text{match}}^{\text{GP}}$ as matching temperature. The Hauser-Feshbach rates are adopted from the code NON-SMOKER [8]. The listed rate ratios apply to $T \geqslant T_{\text{match}}^{\text{ETER}}$.

[f]Ratio of extrapolated reaction rates using $T_{\text{match}}^{\text{ETER}}$ and $T_{\text{match}}^{\text{GP}}$ as matching temperature. The Hauser-Feshbach rates are adopted from the code MOST [9]. The listed rate ratios apply to $T \geqslant T_{\text{match}}^{\text{ETER}}$.

becomes unimportant. (The γ-ray partial width is smaller in magnitude than either of the particle partial widths and thus is negligible in this context.) Because the α-particle appears in the exit, not entrance, channel (i.e., it is not emitted with a thermal energy distribution), it follows that a Gamow peak does not exist for (p,α) reactions at higher energies. Thus, depending on the circumstances, the ETER may be located at higher or at lower energies compared to the Gamow peak.

Although we have shown above that the actual temperature for matching experimental and Hauser-Feshbach rates is significantly higher than previously assumed, we have not demonstrated yet that the *extrapolated* recommended rates (i.e., in the region beyond the matching temperature) will change as well. It must be remembered that the absolute value of the Hauser-Feshbach rate is of no concern here. The fact that Hauser-Feshbach rates are matched to experimental results implies that, concerning the absolute magnitude of the reaction rate, the latter results are clearly preferred over the former *if a set of measured resonances is available*. What is of main interest for the matching procedure is the *temperature dependence* of the Hauser-Feshbach rate. If experimental and Hauser-Feshbach reaction rates have similar temperature dependences at high temperatures, then it obviously does not matter at which temperature both rates are matched: the same extrapolated rates are obtained if the matching is performed at $T_{\text{match}}^{\text{ETER}}$ or $T_{\text{match}}^{\text{GP}}$. Thus we only expect to obtain differences in extrapolated rates if the temperature dependence of experimental and Hauser-Feshbach rates is different.

For all reactions listed in Table I we extrapolated the rates to high temperatures, first based on our new matching temperature, $T_{\text{match}}^{\text{ETER}}$, and then repeated the calculation using the Gamow peak concept, $T_{\text{match}}^{\text{GP}}$. The ratio of the resulting rates (at temperatures beyond $T = T_{\text{match}}^{\text{ETER}}$) is given in two columns in Table I: columns 6 and 7 have been obtained using the Hauser-Feshbach computer codes NON-SMOKER [8] and MOST [9], respectively. It can be seen that for 15 of 21 investigated reactions the rate ratios exceed 50% for at least one of the Hauser-Feshbach models, implying that a matching of reaction rates at $T_{\text{match}}^{\text{ETER}}$ instead of $T_{\text{match}}^{\text{GP}}$ has a significant effect on the extrapolated results. The largest variations are obtained

for ^{32}S$(p,\gamma)^{33}$Cl (factor 14) and ^{36}Ar$(p,\gamma)^{37}$K (factor 7). It is also apparent that for many reactions the rate ratios listed in columns 6 and 7 disagree by large factors, indicating that the NON-SMOKER and MOST rates have different temperature dependences. We leave a more thorough investigation to future work.

Finally, we would like to discuss the results of an important test. It will not have escaped the attention of the careful reader that the location of the ETER, as defined in Sec. II, depends on the experimental cutoff energy $E_{\rm max}^{\rm exp}$. Clearly, resonances are missing at the high-energy end of the fractional rate distribution and this circumstance will influence the values of the derived 8th, 50th, and 92nd percentiles of the cumulative distribution (Fig. 4). We expect that the "true" ETER (which would take into account *all* resonances) will generally be located at higher energies compared to our calculated ETER (which is based on an experimental set of resonances that is truncated at $E_{\rm max}^{\rm exp}$). Among all cases listed in Table I, the ^{27}Al$(p,\gamma)^{28}$Si reaction has the highest value of $E_{\rm max}^{\rm exp}$. We may use this observation for investigating the sensitivity of our calculated (truncated) reaction rates on the experimental cutoff energy. The results are displayed in Fig. 6. Suppose that we would artificially truncate the fractional rate distribution for 105 resonances at an energy of 1.0 MeV so that only the 26 lowest-lying resonances are taken into account. The resulting matching temperature, calculated from Eq. (6), would amount to $T_{\rm match}^{\rm ETER} = 0.94$ GK (displayed at the top of the two vertical bars in the figure). The (truncated) ETER would then be located at $E = 333$-740 keV (open black vertical bar). This can be compared to the location of the (full) ETER, $E = 334$–741 keV, calculated at the same temperature taking all 105 resonances up to $E_{\rm max}^{\rm exp} = 3.8$ MeV into account. The total reaction rates increase by only 1% as a result of considering the full (105 resonances) versus the truncated (26 resonances) distribution. Clearly, the effect of truncating the actual distribution of fractional rate contributions on the resulting total reaction rate is very small. Similar results (maximum variations of ≈10%) have been obtained at higher artificial experimental cutoff energies, as is apparent from the results displayed in Fig. 6, and by repeating this test using the ^{26}Mg$(p,\gamma)^{27}$Al reaction which has the largest number of resonances among all cases listed in Table I. The tests also show that a value of $n = 1$ for the empirical parameter in Eq. (6) provides sufficiently accurate results. Thus we are confident that our method reliably predicts the effective thermonuclear energy range for charged-particle thermonuclear fusion reactions.

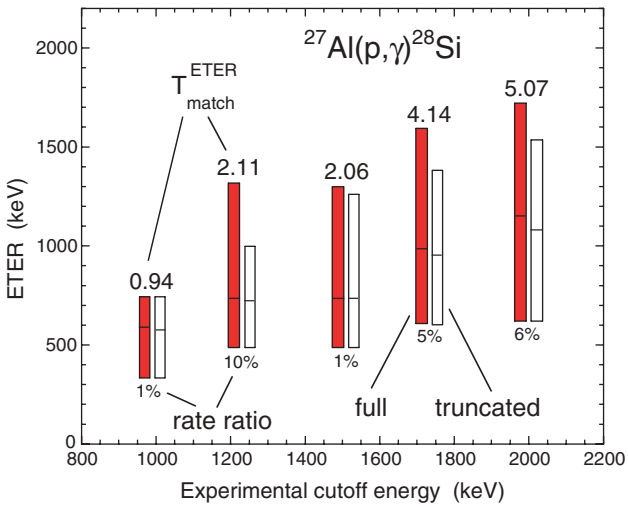

FIG. 6. (Color online) Effect of truncating the fractional distribution of narrow resonance contributions on the ETER for the reaction ^{27}Al$(p,\gamma)^{28}$Si. See text. The x axis displays an artificial experimental cutoff energy. The numbers at the top of the vertical bars correspond to $T_{\rm match}^{\rm ETER}$ (in GK) calculated from Eq. (6) by using a value of $n = 1$. The open black vertical bars show the ETER computed at $T_{\rm match}^{\rm ETER}$ for the artificial cutoff energy displayed on the x axis, whereas the solid red vertical bars display the ETER calculated at the same temperature using the full set of experimentally known resonances up to an energy of $E_r = 3.8$ MeV. In both cases the ETERs are defined by the 8th, 50th, and 92nd percentiles of the cumulative distribution of fractional resonance rate contributions (Sec. III). The percentage number at the bottom of the vertical bars indicates the amount of variation in the total reaction rate caused by the artificial experimental cutoff energy.

IV. SUMMARY

The present work describes a new method for matching experimental and Hauser-Feshbach reaction rates at high temperatures ($T > 1$ GK). Reliable reaction rates at such temperatures are required for studies of advanced stellar burning stages, supernovae, and x-ray bursts. The method employs the actual experimental distribution of fractional resonant rate contributions to the total rate. We define an *effective thermonuclear energy range* (ETER) by using the 8th, 50th, and 92nd percentiles of the corresponding cumulative distribution. It is demonstrated that this energy range differs significantly from the commonly used Gamow peak region. The differences are explained by the vastly different energy dependences of the entrance and exit channel partial widths of resonances. Our ideas are applied to 21 (p,γ), (p,α), and (α,γ) reactions on $A = 20$–40 target nuclei. Based on the ETER we generally find a matching temperature that deviates significantly from previous values that were based on the Gamow peak. Furthermore, for many cases studied here, our extrapolated reaction rates at high temperatures differ significantly from those obtained using the Gamow peak concept. The full impact of our work on a larger set of reactions will be addressed in a future study.

ACKNOWLEDGMENTS

The authors are grateful to Thomas Rauscher and Stephane Goriely for providing their Hauser-Feshbach reaction rates. The comments of Ryan Fitzgerald are highly appreciated. This work was supported in part by the U.S. Department of Energy under Contract No. DE-FG02-97ER41041.

[1] C. Iliadis, *Nuclear Physics of Stars* (Wiley-VCH, Weinheim, 2007).
[2] C. Angulo *et al*., Nucl. Phys. **A656**, 3 (1999).
[3] C. Iliadis, J. M. D'Auria, S. Starrfield, W. J. Thompson, and M. Wiescher, Astrophys. J. Suppl. Ser. **134**, 151 (2001).
[4] W. A. Fowler and F. Hoyle, Astrophys. J. Suppl. **9**, 201 (1964) app. C.
[5] J. R. Newton, C. Iliadis, A. E. Champagne, A. Coc, Y. Parpottas, and C. Ugalde, Phys. Rev. C **75**, 045801 (2007).
[6] P. M. Endt, Nucl. Phys. **A521**, 1 (1990).
[7] P. M. Endt, Nucl. Phys. **A633**, 1 (1998).
[8] T. Rauscher and F.-K. Thielemann, At. Data Nucl. Data Tables **75**, 1 (2000).
[9] M. Arnould and S. Goriely, Nucl. Phys. **A777**, 157 (2006).